

Review

# Characteristics and Applicability Analysis of Nanomorphological Structures for Chemosensors: A Systematic Review

Hye-Ree Han

Department of Beauty Art Care, Graduate School of Dongguk University, Seoul 04620, Republic of Korea; luckyherry@hanmail.net

**Abstract:** The necessity for complex functionality materials is increasing due to the emergence of high-tech technologies and the deepening needs of B-to-B companies in the industry. Study on advanced multifunctional materials is also increasing due to interest in fields such as the Internet of Things (IOT), Fourth Industrial Revolution, and artificial intelligence (AI). Nanomaterials have the advantage of having a large surface area, making it easier to express more efficient properties, and they have been widely applied recently in various fields. When designing new materials for specific applications, it is often important to control the shape, size distribution, surface properties, dispersion, and agglomeration stability of synthetic nanoparticles, as well as the elemental and nanocrystalline compositions of the materials. Nanomaterials have infinite potential, but there are not many cases of collection and structural classification. Therefore, I attempted to conduct an in-depth systematic review by categorizing nanomaterials into nanoparticles, nanoplates, nanowires, and nanorolls according to their nanostructures. Additionally, the representative materials of nanowires include CuNW (copper nanowire), AgNW (silver nanowire), and GaAsP single nanowire. Moreover, nanoroll-type materials include SWCNTs (single-walled carbon nanotubes), DWCNTs (double-walled carbon nanotubes), and MWCNTs (multi-walled carbon nanotubes). In conclusion, this study, through a systematic review, is intended to provide a cornerstone for application plans when designing cutting-edge chemosensors.

**Keywords:** nanowire; morphological characteristics; nanograin; nanoplate; chemosensors



**Citation:** Han, H.-R. Characteristics and Applicability Analysis of Nanomorphological Structures for Chemosensors: A Systematic Review. *Chemosensors* **2023**, *11*, 537. <https://doi.org/10.3390/chemosensors11100537>

Academic Editor: Pi-Guey Su

Received: 22 August 2023

Revised: 4 October 2023

Accepted: 10 October 2023

Published: 12 October 2023



**Copyright:** © 2023 by the author. Licensee MDPI, Basel, Switzerland. This article is an open access article distributed under the terms and conditions of the Creative Commons Attribution (CC BY) license (<https://creativecommons.org/licenses/by/4.0/>).

## 1. Introduction

In recent years, the importance of nanotechnology has become prominent in this era, where cutting-edge technologies, such as secondary batteries, batteries, and artificial intelligence, are in the spotlight. Nanotechnology, in particular, is a state-of-the-art ultrafine processing technology that requires a level of precision of one billionth of a meter. This has created new technology areas by horizontally connecting existing material fields, inducing synergy between existing academic fields and human resources, and contributing to minimization and performance improvements. In addition, it enables the exploration of the ultrafine world, which has been unknown thus far, and enables the manufacture of new materials, such as those needed for the cloning of animals and plants, using DNA structures and steel fibers. In the field of electronic engineering, the precision of nanometers is required, and, if this is realized, manufacturing technologies such as large-scale integrated circuits (LSIs) are expected to improve dramatically. Many nanomaterials are dispersed in the form of nanoparticles. However, other materials can also use nanostructures within them. For example, metal–organic skeletons can incorporate nanovoids into crystal structures and become host carriers for high concentrations of other molecules. These include active pharmaceutical components. When metal–organic skeletons are dispersed as nanoparticles in biocompatible fluids, they can access cells through surface changes and then release a variety of active and targeted drugs directly, where needed, in the body. Nanomaterials that have recently been in the spotlight include TiO<sub>2</sub>, metal nanowires

(Cu, Ag, etc.), graphene, SWCNTs, DWCNTs, and MWCNTs, along with various other nanomaterials that are being studied [1–13]. Nanomaterials are already used in the form of synthetic nanoparticles in various consumer products, such as textiles, paints, sunscreen, and other medical products. In addition, in-depth research is being conducted to utilize nanomaterials in numerous applications, including energy storage and energy conversion, pharmaceuticals, life sciences, solar cells, catalysts, and synthetic materials. Nanoparticle analysis devices are listed in Table 1.

**Table 1.** List of nanoparticle analysis devices.

Device	Analysis Method	Relevant Literature
FE-SEM (field emission scanning electron microscopy)	Surface photography for the structure, size, etc., of a sample	[14]
AFM (atomic force microscopy)	Photographing the structure and size of a sample in three dimensions	[15]
Dynamic light scattering (DLS), electrophoretic light scattering (ELS), and laser diffraction (LD)	Identifying and verifying the size and behavior of nanoparticles in liquids	[16]
Small-angle X-ray scattering (SAXS) and wide-angle X-ray scattering (WAXS)	Combining information about the shape and size of nanoparticles with all existing nanocrystal structural analyses	[17]
High-resolution X-ray diffraction (HR-XRD) and X-ray reflectivity (XRR)	Used to investigate ‘two-dimensional’ nanolayers	[18]
X-ray fluorescence (XRF)	Analyzing the elemental composition of nanoparticles to evaluate parameters such as doping agent concentration or impurities	[19]
Nanoparticle tracking analysis (NTA)	Used as a tool in nanotoxicology studies for nanoparticle concentration measurements; it can also be used to investigate whether certain samples can be classified as nanomaterials	[20]

When designing new materials for specific applications, it is often important to control the size distribution, shape, surface properties, dispersion, and agglomeration stability of synthetic nanoparticles, as well as the elemental and nanocrystalline compositions of the materials. Therefore, I aimed to conduct an in-depth systematic review by categorizing materials into nanoparticles, nanowires, nanoplates, and nanorolls according to their nanostructures. Additionally, by conducting this review, it was intended that I would provide a cornerstone for the application plans of new chemosensor nanomaterials being designed.

## 2. Methods

Recent studies on applying nanotechnology include chromic materials, metal fibers, semiconductors, electrospun nanowebs, shape nanoparticle coatings, fiber optics, organic materials, and conductive polymers. In this review, nanomaterials were systematically reviewed according to their nanostructures. Figure 1 shows a PRISMA diagram of the research identified via databases. The literature data were collected using the MDPI, Nature, Web of Science, Harvard.edu, ACS, IOP Publishing, Google Scholar, PubMed, SCOPUS, and RISS databases. Keywords used in the literature research were nano, nanowire, nanoplate, nanograin, graphene, SWCNTs, MWCNTs, DWCNTs, etc. Editorials, journals, and artifacts that were irrelevant to the subject were excluded. In addition, 54 selected papers were divided into four configurations (nanograins, nanowires, nanoplates, and nanorolls) and reviewed in depth. In this study, an in-depth review of nanomaterials by structure was conducted using PRISMA techniques. In addition, research was conducted focusing on papers published within the last five years.

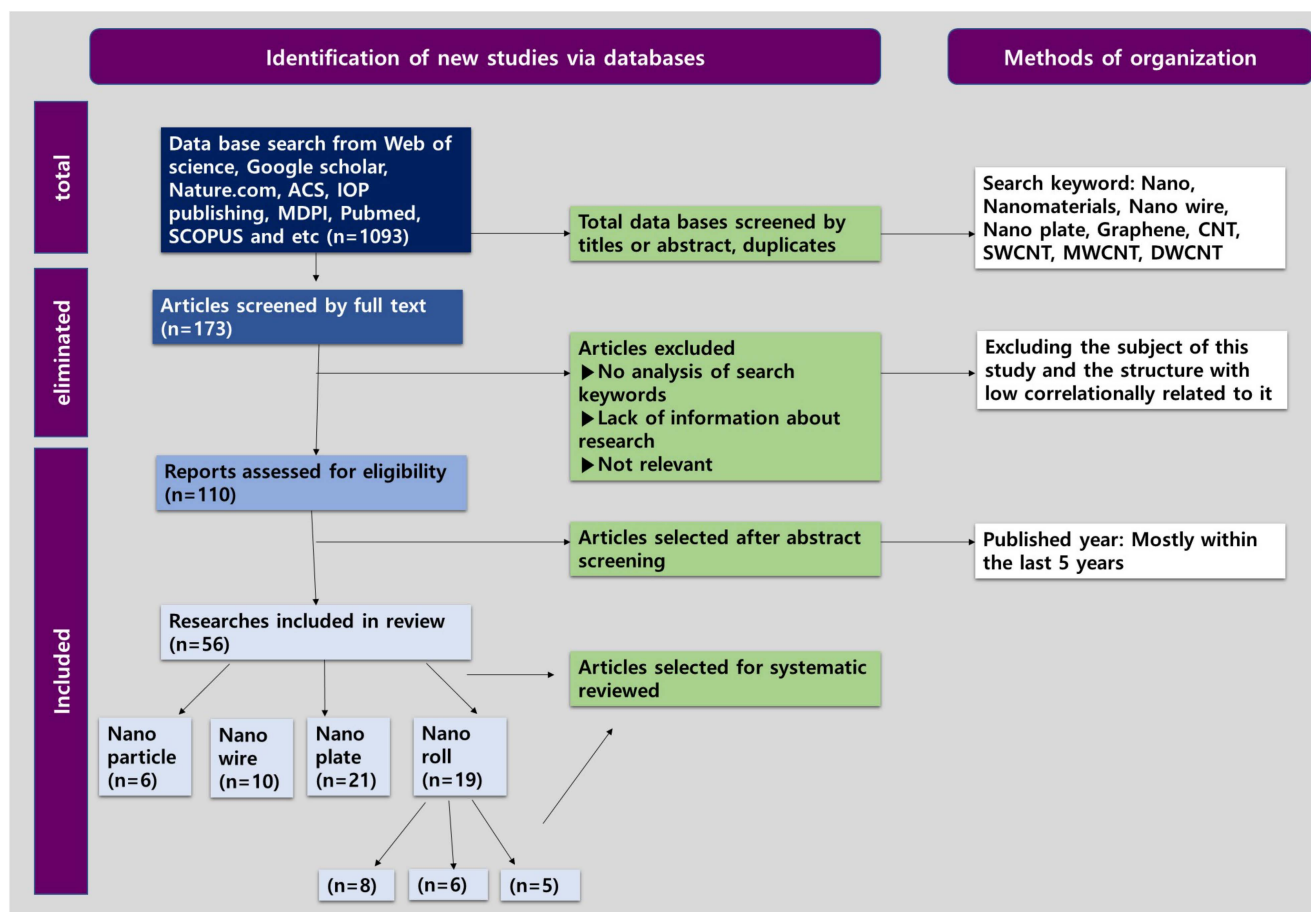


Figure 1. PRISMA diagram of research identified via databases.

The demand for multifunctional materials is increasing due to the recent emergence of high-tech technologies and the increasing needs of B-to-B companies in the industry. Nanomaterials have a large surface area, but there is not a great deal of data to collect and systematically classify, nor are there extensive amounts of data on hybrid nanomaterials and production technologies to organize. Therefore, in this review, nanomaterials were structurally divided and examined in depth.

### 3. Nanomaterials

#### 3.1. Nanoparticles

Nanoparticle refers to ultrafine particles whose unit of size is one billionth of a meter. Nanoparticles are a type of particle, belonging to the domain of nanotechnology, that manipulate molecules or atoms to create new materials, structures, machines, equipment, and devices; further, there have been studies conducted on their structures. Research materials related to nanoparticles include polymer nanoparticles, silica particles, large-pore mesoporous silica nanoparticles, sulfur compounds, etc. [21–26]. Nanoparticles, unlike linear nanowires, have a relatively round circular shape. Due to their large surface area, they exhibit stronger efficacy than microparticles in terms of antimicrobial properties and strength. There are cases in which nanoparticles are used to study the application of nanomaterials in drug delivery, photolysis, tensile strength improvement, regenerative treatment, oxidation catalysts, supercapacitors, energy storage devices, etc. A systematization of nanoparticle articles with bibliographic sources is detailed in Table 2.

**Table 2.** Systematization of nanoparticle articles.

Title	Main Content	Applicability	Relevant Literature
Nanomaterials for Drug Delivery and Cancer Therapy	Drug dynamic profiles, custom applications	Drug vector	Nicoletta et al. [27]
Developing Mg-Gd-Dy-Ag-Zn-Zr Alloy with High Strength via Nano-Precipitation	Mg-10Gd-4Dy-1.5Ag-1Zn-0.5Zr	Metal nanoparticle-based sensors	Xie et al. [28]
Plant-Derived Exosome-like Nanoparticles for Biomedical Applications and Regenerative Therapy	Plant-derived exosome-like nanoparticles	Biofunctionalization, bioink printing, and microfluidic system	Sarasati et al. [29]
A Novel Hydro-Thermal Synthesis of Nano-Structured Molybdenum-Iron Intermetallic Alloys at Relatively Low Temperatures	MoFe and MoFe <sub>3</sub> intermetallic alloys	Metal nanoparticle-based sensors	El-Geassy et al. [30]
Enhancing Drought Tolerance in Wheat Cultivars through Nano-ZnO Priming by Improving Leaf Pigments and Antioxidant Activity	ZnO NPs	Biologically viable strategy, metal oxide nanoparticle-based sensors	Abbas et al. [31]
Construction and Enhanced Efficiency of Bi <sub>2</sub> MoO <sub>6</sub> /ZnO Compo-Sites for Visible-Light-Driven Photocatalytic Performance	Bi <sub>2</sub> MoO <sub>6</sub> /ZnO	Electrochemical sensors, metal oxide nanoparticle-based sensors, photocatalyst	Yan et al. [32]

In recent decades, interest in nanoparticle applications has rapidly increased in various fields, including in electrochemical sensors, drug vectors, metal oxide nanoparticle sensors, photocatalysts, etc.

Polymer, metal, silica, carbon, and hybrid nanoparticles are different types of nanomaterials and are currently used in disease treatment, as well as in many other applications. Nanoparticles are often able to provide suitable features for providing nanoformulations with improved performance, including good drug dynamic profiles and processing efficiency in custom applications. This study can be applied to cancer therapy, chemosensors, biomedical applications, etc. [27]. In a prior study, a high yield strength (~396 MPa) and ultimate tensile strength (~451 MPa) were obtained after high-temperature extrusion and aging, which was achieved by designing a Mg-10Gd-4Dy-1.5Ag-1Zn-0.5Zr alloy via the multielement composite addition method. The potential and fine particles introduced by the extrusion process accelerated the precipitation rate of nanostructures, improving aging curing efficiency, as well as promoting the formation of more uniform and finer nanoconditions. Accordingly, prior research has suggested that introducing nanodeposit networks into fine structures is an effective strategy for developing high-strength Mg alloys. In this research, high-strength Mg alloys, high hardness, etc., can be realized [28]. Another previous study investigated plant-derived exosome-like nanoparticles (PDENs) that consist of a variety of bioactive biomolecules. As an alternative cell-free treatment method, there is the potential to deliver nanocompounds to the human organism. This, therefore, leads to various antioxidant, anti-inflammatory, and antitumor benefits. The preceding study aimed to verify the biomedical potential of PDENs, especially in regenerative therapy applications, by analyzing the latest R&D data.

Through this study, restraining cellular death, initiating bone formation, etc., can be realized [29]. El-Geassy et al. synthesized nanostructured Mo/Fe intermetallic metals from precursors containing 72/28% and 30/70% Mo/Fe molar ratios, which were represented as precursors A and B. These precursors were prepared from a coprecipitation of ammonium heptamolybdate tetrahydroxide and a hot aqueous solution of iron oxalate. In addition, mathematical formulas derived from the gas–solid reaction model were ap-

plied to identify reduction mechanisms that depend heavily on reduction temperature and precursor composition.

They also reported that the gas–solid reaction technology at low temperatures could successfully manufacture nanostructured MoFe and MoFe<sub>3</sub> intermetallic alloys. Through this study, possibilities such as environmentally friendly approaches, the synthesis of binary and tertiary metal alloys, etc., can be seen [30]. As mentioned above, nanoparticles have various advantages due to their structural characteristics; thus, their applicability in various industries is endless. They are widely used in the manufacturing of chemosensors, biochips, displays, and ultrasmall biosensors because they exhibit unusual and diverse properties due to their small size. Furthermore, it is believed that they can be actively applied in the convergence industry. As mentioned above, nanoparticles are expected to be applicable in metal nanoparticle-based sensors, biofunctionalization, metal oxide nanoparticle-based sensors, electrochemical sensors, and photocatalysts.

### 3.2. Nanowire

Nanowire is one of the top 10 new technologies that will change the world and is currently considered one of the most efficient fields in nanotechnology. Nanowires refer to wire structures with a nanometer size. In the microworld, the influence of quantum mechanical effects is dominant, so these wire structures are sometimes called quantum wires. The term generally refers to nanowires with diameters of less than 10 nm to hundreds of nanometers. There is no particular limitation in the length direction of a nanowire. Nanowires are used in various fields, such as lasers, chemical sensors, transistors, and memory. The materials used include semiconductor silicon (silicon), chemically sensitive tin oxide, and gallium nitride (which is a light-emitting semiconductor). Research materials related to nanowires include nanowire Ni–Pd mixed-metal complexes, GaAs nanowires, Ta/InAs nanowires, Cu nanowires, silver nanowires, Ag-Doped CuV<sub>2</sub>O<sub>6</sub> nanowires, etc. [33–38]. A systematization of nanowire journals with bibliographic sources is listed in Table 3.

Yalcin et al. used cryogenic electron microscopy with multimodal functional images and a series of electrical, biochemical, and physiological studies. They also found that nanowires consist of cytochrome OmcZ and OmcS, which transmit electrons through a smooth stacking of hems across micrometers. This study can be applied to bioenergy, biofuels, sensing, synthesis, bioelectronics, and energy production [39]. Jin Huijin et al. reported the rational design and synthesis of anisotropic mesoporous Pt<sub>3</sub> Ni core–shell-structured nanowires for high-efficiency electrocatalysts. These catalysts have been specifically described as having a uniform core–shell structure with a jagged Pt nanowire core of a thin atom and a mesoporous Pt-skin Pt<sub>3</sub> Ni framework shell. They have also been described to have stability, Pt utilization efficiency, and high electrocatalytic activity [40]. Wakizaka Masanori et al. used insulators such as 1D Mott for [Ni(chxn)<sub>2</sub> Br] Br<sub>2</sub> (1; chxn = 1 R-2 R-diaminocyclohexane). This is expected to be the first case of electrochemical liquid epitaxy applied in molecular-based heterostructures on a macroscopic scale.

In addition, atomic-resolution scanning tunneling microscopic images represent electronic state modulation in heterojunction regions with a length of five metal atoms (~2.5 nm). It was argued that this study was the first to show the heterojunction of 1D chains experimentally and investigate them on a macroscopic and atomic scale [41].

Leilei Gu and others produced electrochemical eyes with a hemispherical retina consisting of a high-density array of nanowires mimicking the photoreceptors in the human retina. The device design was structurally very similar to the human eye with the potential for high image resolution when handling individual nanowires electrically.

**Table 3.** Systematization of nanowire articles.

Title	Main Content	Applications	Relevant Literature
The blind men and the filament: understanding structures and functions of microbial nanowires	OmcS, OmcZ	Conducting polymer	Yalcin et al. [39]
Mesoporous Pt@Pt-skin Pt <sub>3</sub> Ni core-shell framework nanowire electrocatalyst for efficient oxygen reduction	Pt <sub>3</sub> Ni	Biosensors, pH sensors	Jin et al. [40]
Macro- and atomic-scale observations of a one-dimensional heterojunction in a nickel and palladium nanowire complex	[Ni(chxn) <sub>2</sub> Br] <sub>2</sub>	Metal nanowire-based sensors	Wakizaka et al. [41]
A biomimetic eye with a hemispherical perovskite nanowire array retina	Mimic photoreceptors in the human retina	Metal nanowire-based sensors	Gu et al. [42]
Porous carbon nanowire array for surface-enhanced Raman spectroscopy	Porous carbon nanowires	Electrochemical image sensor, nanowire photosensors, a hemispherical image sensor	Chen et al. [43]
Transmission phase read-out of a large quantum dot in a nanowire interferometer	One-dimensional networks and demonstrated interferometer readings in nanowire-based architectures	Excellent biocompatibility	Borsoi et al. [44]
Surface-passivated GaAsP single-nanowire solar cells exceeding 10% efficiency grown on silicon	GaAsP single-nanowire solar cell, energy bandgap	Viable tool for parity read-out of future topological qubits	Holm et al. [45]
Electronically stabilized nanowire growth	Self-assembled metal iridium nanowires grown on the surface of germanium (001)	Single-nanowire solar cells	Mocking et al. [46]
Micro-scale fusion in dense relativistic nanowire array plasmas	A string-level pulse of a small ultrafast laser, plasma	Nanowire-based electrochemical sensors	Curtis et al. [47]
Anomalous high capacitance in a coaxial single nanowire capacitor	Coaxial asymmetric Cu–Cu <sub>2</sub> OC structure	Ion-tracked polycarbonate	Liu et al. [48]

We also demonstrated the image detection capabilities of biomimetic devices by reconstructing the optical patterns projected on the device. It was argued that this work could lead to biomimetic light sensing devices becoming available in a wide range of technical applications. This study shows the possibilities of a wide spectrum of technical applications, biomimetic photosensing devices, etc. [42]. Nan Chen et al. demonstrated the design, manufacture, and use of metal-free (i.e., LSPR-free) topological custom nanostructures consisting of porous carbon nanowires arranged as SERS substrates. They explained that due to their high signal enhancement (~106) and strong broadband charge transfer resonance, there was no hotspot; thus, they are highly reproducible, nonoxidized, and highly compatible with biomolecules due to their high durability and fluorescence dissipation capability [43]. Francesco Borsoi et al. leveraged recent breakthroughs in the growth of one-dimensional networks and demonstrated interferometer readings in nanowire-based architectures. In this study, Fano resonance caused by interference between electrons moving through the reference arm and electrons experiencing resonance tunneling at quantum dots was observed. Additionally, these results provide important insights into future topology qubit designs. This study shows the characteristics of viable tools for parity read-out of future topological qubits in nanowire networks [44]. Jeppe V. Holm et al. explained that today's need for lattice matching limits bandgap combinations that can be used in

multijunction solar cells and prohibits the monolithic integration of low-cost silicon solar cells and high-efficiency III-V materials. In addition, the use of III-V nanowires is the only known way to bypass these lattice-matching constraints. Therefore, the study argued that it is necessary to develop the growth of nanowires with bandgaps of  $>1.4$  eV. Accordingly, they presented the first gold-free gallium arsenic phosphide nanowires that were grown in silicon through direct epitaxial growth. They also demonstrated that their bandgap could be controlled during growth and in manufactured core-shell nanowire solar cells [45]. Tijds F. Mockinge et al. [46] explained that metal nanowires exhibit unique physical characteristics due to their one-dimensional characteristics. Most of these characteristics are related to electron interaction. And in this study, it was noted that electron interaction plays a much more important role in one dimension.

This research explains the unique physical properties of these materials in terms of their one-dimensional nature and the presence of electron standing-wave patterns in the nanowires. Alden Curtis et al. explained that fusion is regularly generated from spherical plasma compression that is driven by multikilojoule pulses of the world's largest laser. In addition, the investigation of deuterated polyethylene nanowire arrays aligned with femtosecond pulses of relativistic strength explained that deuterium (D) produces ultrahigh-energy-density plasma that accelerates up to MeV energy [47].

Zheng Liu et al. researched a single-nanowire capacitor with a coaxial asymmetric Cu-Cu<sub>2</sub>O structure. Samples were manufactured using a two-step vapor deposition method and a chemical reaction method. And the capacitance measured on a nanowire device corresponded to  $\sim 140 \mu\text{F cm}^{-2}$ .

Therefore, it has been reported to exceed the previously reported value of the metal-insulator-metal microcapacitor and to be 10 times higher than that which was previously detected by classical static electricity [48]. In addition, nanowires have various advantages due to their linear structure and are applied in various industrial fields. It is believed that nanowires could be applied in high-tech industries, e.g., in transparent electrodes, high current binders, EV batteries, and displays. As mentioned above, nanowires are expected to be applicable in conducting polymer-based sensors, biosensors, pH sensors, metal nanowire-based sensors, electrochemical image sensors, nanowire photosensors, hemispherical image sensors, etc.

### 3.3. Nanoplates

Nanoplates are plate-shaped nanostructures. Graphene has a large surface area due to its wide plate shape. Studies related to nanoplates include graphene, an Au nanoplate, a polypyrrole-modified  $\text{NH}_4\text{NiPO}_4 \cdot \text{H}_2\text{O}$  nanoplate, a  $\text{LiMnPO}_4$  nanoplate,  $\text{Bi}_2\text{Te}_3$ ,  $\text{Bi}_2\text{Se}_3$  nanoplates and etc. [49–52]. A systematization of nanoplate journals with bibliographic sources is listed in Table 4.

**Table 4.** Systematization of nanoplate articles.

Title	Main Content	Applications	Relevant Literature
Visible Surface Plasmon Modes in Single $\text{Bi}_2\text{Te}_3$ Nanoplate	$\text{Bi}_2\text{Te}_3$ nanoplate	Metal nanoplate-based sensors	Meng et al. [53]
Surface-Plasmon-Mediated Programmable Optical Nanofabrication of an Oriented Silver Nanoplate	Silver nanoplate	Thermoelectric sensors	Bin et al. [54]
Layered $\text{Bi}_2\text{Se}_3$ Nanoplate/Polyvinylidene Fluoride Composite Based n-type Thermoelectric Fabrics	$\text{Bi}_2\text{Se}_3$ nanoplate/polyvinylidene fluoride composite	Metal nanoplate-based sensors	Chao et al. [55]
Norbert F. S. Enhancing Nanoparticle Electrodynamics with Gold Nanoplate Mirrors	Gold nanoplate mirrors	Metal nanoplate-based sensors	Zijie et al. [56]
Gated Hall Effect of Nanoplate Devices Reveals Surface-State-Induced Surface Inversion in Iron Pyrite Semiconductor	Iron pyrite semiconductor	Nanoplate-based electrochemical sensors	Dong et al. [57]

Table 4. Cont.

Title	Main Content	Applications	Relevant Literature
Electrochemical Transparency of Graphene	Graphene	Optical biosensing, environmental sensing	Du et al. [58]
Graphene Photonics, Plasmonics, and Broadband Optoelectronic Devices	Graphene	Nanoplate-based electrochemical sensors	Qiaoliang et al. [59]
A Green Voltammetric Determination of Molnupiravir Using a Disposable Screen-Printed Reduced Graphene Oxide Electrode: Application for Pharmaceutical Dosage and Biological Fluid Forms	Reduced Graphene Oxide	Electrochemical sensors	Nabil et al. [60]
Raman Radiation Patterns of Graphene	Graphene	Nanoplate-based electrochemical sensors	Harald et al. [61]
Electronic Properties of Nanodiamond Decorated Graphene	Graphene	Semiconducting nanoplate-based sensors	Yu et al. [62]
Controlled Growth of Semiconducting Nanowire, Nanowall, and Hybrid Nanostructures on Graphene for Piezoelectric Nanogenerators	Graphene	Graphene–TMD bilayer heterostructure-based photodetectors	Brijesh et al. [63]
Hybrid Heterostructures to Generate Long-Lived and Mobile Photocarriers in Graphene	Graphene	Electrochemical sensors	Pavel et al. [64]
Highly Deformable Graphene/Poly(3,4-ethylenedioxythiophene):Poly(styrene Sulfonate) Hydrogel Composite Film for Stretchable Supercapacitors	Graphene/poly(3,4-ethylenedioxythiophene):poly(styrene sulfonate) hydrogel composite film	Polymeric and graphene-based sensors, capacitive pressure sensor	Wen et al. [65]
Heil Modeling Graphene–Polymer Heterostructure MEMS Membranes with the Föppl–von Kármán Equations	Graphene–polymer heterostructure MEMS membranes	Electrochemical energy storage	Katherine et al. [66]
Direct-Chemical Vapor Deposition-Enabled Graphene for Emerging Energy Storage: Versatility, Essentiality, and Possibility	Graphene	Energy storage	Zixiong et al. [67]
Ultrafast Terahertz Self-Induced Absorption and Phase Modulation on a Graphene-Based Thin Film Absorber	Graphene-based thin-film absorber	Terahertz radiation	Anastasios et al. [68]
Graphene Hydrogel as a Porous Scaffold for Cartilage Regeneration	Graphene	Biopolymers, scaffolds	Chengqi et al. [69]
Mesoscopic Klein-Schwinger effect in graphene	Graphene	Nanoplate-based electrochemical sensors	Schmitt et al. [70]
Observation of hydrodynamic plasmons and energy waves in graphene	Graphene	Nanoplate-based electrochemical sensors	Zhao et al. [71]
Unexpectedly efficient ion desorption of graphene-based materials	Graphene	High-efficiency desorption, extraction, and concentration of ions with potential applications	Xia et al. [72]
Enhanced superconductivity in spin–orbit proximitized bilayer graphene	Spin–orbit proximitized bilayer graphene	Nanoplate-based electrochemical sensors	Zhang et al. [73]

Meng Zhao et al. reported that solution-synthesized hexagonal  $\text{Bi}_2\text{Te}_3$  nanoplates without lattice configurations can exhibit multiple plasmon modes in transmission electron microscope-based electron energy-loss spectroscopy and cathode emission spectroscopy. Theoretical calculations show that the observed plasmon in the visible range is mainly due to the strong spin–orbit coupling that induces the metal surface state of  $\text{Bi}_2\text{Te}_3$ . This research shows advancement in the field of plasmonics, with strong spin–orbit coupling-induced metallic surface states of  $\text{Bi}_2\text{Te}_3$  [53]. Bin-Bin et al. reported polarized femtosecond laser light-mediated growth and the programmable assembly of silver nanoparticles reduced to triple-layer fine patterns. In addition, the growth mechanism of nanoplates became clear. The excited surface plasmon enhanced the local electric field and induced the spatial selective growth of the silver atom at the opposite end of the dipole, which induced the

initially produced silver seed. Optical attraction overcoming electrostatic repulsion in enhanced local electricity is a field of industry that assembles nanoparticles directly. The shape and position of the triple hierarchical fine pattern, as well as the nanoplate orientation and thickness, are all achieved in a controlled manner [54]. Chao Chao et al. studied layered Bi<sub>2</sub>Se<sub>3</sub> nanoplate/polyvinylidene fluoride composites. In addition, using these, an in-depth study was conducted on the manufacture of n-type flexible thermoelectric fabrics. In this study, the composite showed room-temperature Seebeck coefficient and electrical conductivity values of  $-80 \mu\text{V K}^{-1}$  and  $5100 \text{ Sm}^{-1}$ , respectively. These composites are likely to be used in general applications of thermoelectric devices where light and flexible materials can be useful. This study shows the applicability of high-performance thermoelectric fabrics, the excellent durability of the thermoelectric fabrics, topological insulators, etc. [55].

Zijie Yan et al. explained that synthesized Au nanoplates have the potential to serve as micrometer-sized mirrors that enhance electrodynamic interactions. In other words, the Au nanoplates improve the brightness of light scattered from Ag nanoparticles near the nanoplate surface measured by a dark-field microscope due to their plasmonic properties. In addition, the improvement in the interparticle force constant was found to be more than 20 times higher than expected for the increase in intensity due to steady-wave interference. They showed that additional stability for optical coupling occurs in the limited heat storage motion of nanoparticles, which binds to fluctuations in the lateral plane and decreases [56]. Dong Liang et al. first developed a general method for completely characterizing surface inversion and bulk electrical transfer properties through electrolyte gate hole measurement of explosive nanoplate devices achieved using high surface-to-bulk ratios and effective electrolyte gating in nanostructures. Their work is n-type and p-type near the surface by a strong inversion of sulfur light. And it shows that it yields both the concentration and mobility of bulk electrons and surface holes. In addition, the solution of the Poisson equation shows high-density surface holes that are deposited in a strong inversion layer with a thickness of 1.3 nm and an upward band bending of 0.9–1.0 eV. In this study, the bulk and surface transfer properties of semiconductors are studied, and a general methodology using nanostructures' transfer measurements is presented. This research shows surface inversion, bulk electrical transport properties, etc. [57]. Using the electrochemical transparency of graphene, Jung Doo-won and others showed that the prerequisite for the redox reaction of Prussian blue (PB) is not the direct interlayer insertion of alkali metal cations. The PB thin film that was immobilized with single-layer graphene still had alkali metal ion (K<sup>+</sup> or Na<sup>+</sup>) cations penetrating the graphene that could not be included in the PB. Graphene passivation preserves the electrochemical activity of PB and substantially improves the stability of PB [58]. On the other hand, research on graphene is increasing, as the material is in the form of a representative nanoplate. Graphene is attracting great attention because of its lightweight nature, thinness, durability, excellent thermal conductivity, high electrical conductivity, large Young's modulus, and large specific surface area. Graphene applications include displays, solar cells, optical filters, electronic shielding agents, touch screens, transparent electrodes, seawater desalination filters, high-speed chargers, etc. Graphene-related research includes optoelectronic devices, electrochemical transparency, electronic properties, Raman radiation patterns, piezoelectric nanogenerators, mobile photocarriers, etc. [59–64]. Wen Chen et al. explained that graphene films are widely applied in supercapacitors due to their high electrical conductivity and excellent mechanical strength. However, applications in flexible supercapacitors are still hampered by their low elastic deformation capabilities. Graphene conductive polymer hydrogel (GCPH) composite film may increase to 114.6% of its original length. This research considers the characteristics of ductility, stretchable supercapacitors, etc. [65]. Katherine et al. explained that ultrathin graphene-based membranes showed significant potential for high-performance nanoelectromechanical devices. They presented a graphene–polymer heterostructure (GPH) NEMS membrane model based on the Föppl–von Kármán (FvK) equation, which considered both bending and stretching forces. An experimental GPH membrane shape and FvK-based finite-element method simulation were obtained through atomic microscope topographic mapping. As a result

of comparing the predicted expansion shape, they showed excellent agreement with each other [66]. Zixiong et al. explained that direct chemical vapor deposition (CVD) technology has stimulated tremendous scientific and industrial interest in enabling the isometric growth of graphene on various substrates that easily bypass boring delivery processes and enhance innovative material paradigms. Direct-CVD-capable graphene plays a pivotal role in electrochemical energy storage as it leverages attractive structural advantages and physicochemical properties when compared to typical graphene materials (i.e., reduced graphene oxide and liquid-depleted graphene). This study considers the characteristics of direct growth, versatility, cyclic stability, electrochemical energy storage, etc. [67]. Anatasios et al. presented a thin-film graphene-based THz complete absorption device that can control graphene doping levels through electrostatic gating after plating on the back with single-layer graphene and metal back reflectors placed on an ionic liquid substrate. Their analysis also mapped the temporal dynamics of a THz-induced temperature rise in graphene carriers, thereby explaining the superfast sub-picosecond properties of the entire process. These results can find applications in future dynamically controlled planar optics and in the space–time formation of powerful THz electric fields [68]. Chengqi et al. utilized graphene hydrogels with stable and adjustable structures and model scaffolds to investigate the effect of porous structures on the matrix remodeling that is related to the internal growth of cartilage cells in a scaffold. They observed a much more accelerated but balanced cartilage remodeling that correlates with the internal growth of cartilage cells to graphene scaffolding that has open-pore structures on the surface. This research reveals the characteristics of the cartilage matrix, cartilage regeneration, etc. [69]. Schmitt et al. studied the definitive modification of Schwinger’s effect in graphene that houses Dirac fermions with approximate electron–hole symmetry. In this work, using transmission measurements, they studied universal one-dimensional Schwinger conductivity in pinch-offs of ballistic graphene transistors. As a result of the study, the strong pinch-off field was concentrated within about 1  $\mu\text{m}$  of the transistor drain to induce the creation of Schwinger electron–hole pairs under saturation [70]. Zhao et al. reported observations of hydrodynamic plasmon and energy waves in ultraclean graphene. They used on-chip terahertz (THz) spectroscopy techniques to measure the propagation of energy waves in graphene near the THz absorption spectrum of graphene microribbons and charge neutrality. And the hydrodynamic bipolar plasmon featured inverse phase oscillations of massless electrons and holes in graphene. Their observations opened up new opportunities in this study to explore collective fluid dynamics in graphene systems [71]. Xia et al. experimentally demonstrated fast and efficient ion desorption in magnetite graphene oxides by adding a small amount of  $\text{Al}^{3+}$ . As a result of this study, the corresponding concentration of  $\text{Al}^{3+}$  used was reduced at least 250 times compared to the existing desorption method. For typical radioactive and divalent ions,  $\text{Co}^{2+}$ ,  $\text{Mn}^{2+}$ , and  $\text{Sr}^{2+}$ , the desorption rate reached  $\sim 97.0\%$  within  $\sim 1$  min. The study suggests that the proposed method could be used to enrich a wider range of ions in the fields of materials science, energy, environmental technology, and biology [72]. Zhang et al. showed that deploying single-layer tungsten diselenide ( $\text{WSe}_2$ ) on Bernal-stacked bilayer graphene (BLG) promotes Cooper pairing to an alarming degree. Superconductivity appears in the zero magnetic field and occurs over a  $\text{Tc}8\times$  wider density range. In this work, the quantum oscillations of BLG-WSE 2 are mapped as a function of the electric field and doping to show superconductivity across the region where the steady state is polarized. And they confirm that two of the four spin valley flavors are mainly filled [73].

Nanoplates have various advantages due to their structure and are applied in various fields. Nanoplates are expected to be used in various fields, such as electrically conductive materials, nonflammable foam, and solar energy industries. As mentioned above, nanoplates are expected to be applicable in metal nanoplate-based sensors, thermoelectric sensors, optical biosensing, environmental sensing, electrochemical sensors, semiconductor nanoplate-based sensors, capacitive pressure sensors, etc.

### 3.4. Nanorolls

Nanoroll refers to nanomaterials made into a roll-type structure. Depending on how many roll forms overlap, nanoroll materials are divided into SWCNTs (single-walled nanotubes), MWCNTs (multi-walled nanotubes), and DWCNTs (double-walled nanotubes).

#### 3.4.1. SWCNTs and Their Composites

Single-walled carbon nanotubes (SWCNTs) consist of a two-dimensional hexagonal lattice of carbon atoms and have their own mechanical, electrical, optical, and thermal properties. Research related to SWCNTs includes aerogels, in situ electropolymerization, hybrid films, transistors, sensing, gas sensor, etc. [74–79].

A systematization of SWCNT journals with bibliographic sources is listed in Table 5.

**Table 5.** Systematization of SWCNT articles.

Title	Main Content	Applications	Relevant Literature
Investigating valley-dependent current generation due to asymmetric energy dispersion for charge-transfer from a quantum dot to single-walled carbon nanotube	Single-walled carbon nanotube	SWCNT-based nano electronic circuits	Charoenpakdee et al. [80]
Encapsulation of an anticancer drug Isatin inside a host nano-vehicle SWCNT: a molecular dynamics simulation	Single-walled carbon nanotube	SWCNT-based drug delivery cargo systems	Dehaghani et al. [81]
Revealing the effect of electrocatalytic performance boost during hydrogen evolution reaction on free-standing SWCNT film electrode	Single-walled carbon nanotube	SWCNT-based nano electrochemical sensors	Kordek et al. [82]
Heat diffusion-related damping process in a highly precise coarse-grained model for nonlinear motion of SWCNT	Single-walled carbon nanotube	Heat diffusion	Koh et al. [83]
Long-lived electronic spin qubits in single-walled carbon nanotubes	Single-walled carbon nanotube	SWCNT-based nano electrochemical sensors	Chen et al. [84]
High Thermoelectric and Flexible PEDOT/SWCNT/BC Nanoporous Films Derived from Aerogels	PEDOT/SWCNT/BC	SWCNT-based thermoelectric sensors	Fang et al. [85]
Large-Scale Production of PMMA/SWCNT Composites Based on SWCNT Modified with PMMA	PMMA/SWCNT	Covalent functionalization	Robin et al. [86]
Anisotropic Polyaniline/SWCNT Composite Films Prepared by in Situ Electropolymerization on Highly Oriented Polyethylene for High-Efficiency Ammonia Sensor	Polyaniline/SWCNT	Anisotropic polyaniline/SWCNT composite-based high-efficiency ammonia sensor	Tingcong et al. [87]

SWCNTs may be synthesized with various chiral indices to determine specific properties. This work theoretically investigates the electron transport that occurs in different directions along SWCNTs. The electrons studied in the work of Charoenpakdee et al. move in quantum dots that can move right or left in SWCNTs with different probabilities, depending on the valley. These results show the existence of valley polarization currents. The valleys in the left and right directions have a configuration of valley degrees of freedom in which the components  $K$  and  $K'$  are not the same. These results can be theoretically tracked by certain effects. The performance and effectiveness of nanoscale devices, including artificial antennas, transistors, quantum computers, solar cells, and nano electronic circuits, must be improved in order to achieve a variety of benefits [80]. Dehaghani et al. describe the process of encapsulating isatin (1H-indole-2,3-dione), a common anticancer drug, into guest molecules in capped single-walled carbon nanotube (SWCNT) hosts with chirality (10,10). The encapsulation process was modeled by molecular dynamics (MD) simulations under the standard NVT ensemble, taking into account aqueous solutions. The free energy of the encapsulations was found to be  $-34 \text{ kcal mol}^{-1}$ . This suggested that the isatin

insertion procedure into the SWCNTs occurred spontaneously [81]. Kordek-Khalil et al. explained that single-walled carbon nanotubes are assembled as standalone films. This research was used directly in relation to HER electrodes. During the initial 20 h of the electrocatalytic process under constant current conditions, the film was activated, resulting in a gradual overvoltage reduction to a value of 225 mV. In this study, the transient physicochemical properties of the membrane in various activation stages revealed material properties responsible for improving activity. And the findings show that partial oxidation of iron nanoparticles encapsulated in SWCNTs is a major cause of improved activity. This research shows engineering high-performance and low-cost electrodes, etc. [82]. Koh et al. have shown that the thermal diffusion along the tube axis affects the macroscopic movement of SWCNTs and that applying this phenomenon to the coarse-grained model can exceptionally improve the precision of coarse-grained molecular dynamics. In this study, the nonlinear macroscopic motion of SWCNTs under free-heat oscillation conditions in adiabatic environments was demonstrated in the most simplified CG modeling versions. And CG modeling has been shown to maintain finite temperature and total energy with the proposed dispersion process derived from internal thermal diffusion. The nonlinear dynamic properties of SWCNTs can be reproduced in CG models without ambient temperature regulation [83]. Chen et al. explained that single-walled carbon nanotubes (SWCNTs) are whole-carbon one-dimensional materials with spin-free environments and weak spin-orbit couplings ensuring long spin consistency times. They also explained that SWCNTs provide various degrees of freedom for extended functional ranges that are not available in bulk systems. This research shows the combination of molecular approaches with inorganic crystalline systems, etc. [84]. Fang et al. made a film capable of achieving, at the same time, high electrical conductivity and low thermal conductivity through a post-treatment of bacterial cellulose (BC) SWCNT hybrid aerogel, which was performed in order to synthesize poly(3,4-thylenedioxythiophene) (PEDOT) into SWCNT-nanoporous PEDOT. The film also showed excellent flexibility, a fracture strength of 1.6 MPa, and a fracture elongation of 2.13%. The PEDOT/SWCNT/BC film has broad prospects in wearable thermoelectric applications [85]. Robin et al. redistributed single-walled carbon nanotubes (SWCNTs) and a produced compound into dimethylformamide (DMF). The thermal and mechanical properties of the composite materials were determined by differential scanning calorimetry (DSC), tensile tests, thermal weight analysis (TGA), etc. As a result of studying the SWCNT load at a low place, the tensile properties did not change, while the impact strength improved by 20% [86]. Tingkong et al. manufactured single-walled carbon nanotubes (SWCNTs) and anisotropic composite films of polyaniline (PANI) by field electropolymerization in highly oriented high-density polyethylene (HDPE) films. The film used as a reaction in this study was an SWCNT ammonia sensor [87].

Single-walled carbon nanotubes (SWCNTs) have superior transparency and physical properties when compared to multi-walled CNTs (MWCNTs), consisting of multiple layers of carbon structures and having wide application in fields such as conductive films, polymer compounds, and metal compounds. Additionally, SWCNTs have various advantages due to their structure; thus, it is believed that they can be used in various fields, such as electrically conductive materials, nonflammable foam, and the solar industry. As mentioned above, SWCNTs are expected to be applicable in electrochemical sensors, electrochemical sensors, thermoelectric sensors, etc.

### 3.4.2. DWCNTs and Their Composites

DWCNT (double-walled carbon nanotube)-related studies include energy transfer, neuronal network engineering, optimal heat capacity, high-conductivity flexible electrodes, etc. [88–93].

A systematization of DWCNT journals with bibliographic sources is listed in Table 6.

**Table 6.** Systematization of DWCNT articles.

Title	Main Content	Applications	Relevant Literature
DWCNT-Doped Silica Gel Exhibiting Both Ionic and Electronic Conductivities	Double-walled carbon nanotube	DWCNT-based nano electronic conductive sensors	Benjamin et al. [94]
Efficient Inner-to-Outer Wall Energy Transfer in Highly Pure Double-Wall Carbon Nanotubes Revealed by Detailed Spectroscopy	Double-walled carbon nanotube	DWCNT-based nano electrochemical sensors	Maksiem et al. [95]
Composites of Double-Walled Carbon Nanotubes with bis-Quaterthiophene-Fluorenone Conjugated Oligomer: Spectroelectrochemical and Photovoltaic Properties	Double-walled carbon nanotube	DWCNT-based nano electrochemical sensors	Lionel et al. [96]
Experimental Evidence of a Mechanical Coupling between Layers in an Individual Double-Walled Carbon Nanotube	Double-walled carbon nanotube	DWCNT-based nano electrochemical sensors	Levshov et al. [97]
Field-Effect Characteristics and Screening in Double-Walled Carbon Nanotube Field-Effect Transistors	Double-walled carbon nanotube	DWCNT-based field-effect transistors	Wang et al. [98]
Nonlinear Vibration of Double-Walled Carbon Nanotubes Subjected to Mechanical Impact and Embedded on Winkler–Pasternak Foundation	Double-walled carbon nanotube	DWCNT-based flexible pressure sensor, capacitive pressure-sensing, nanosensors	Herisanu et al. [99]

Benjamin et al. prepared a silica gel that was doped with double-walled carbon nanotubes (DWCNTs), which was achieved by using an aqueous sol–gel pathway under mild conditions. And they studied these two conduction paths, which are dominant in different characteristic time scales. The ion conduction of silica networks was independent of the DWCNT doping rate. The DWCNT networks were found to occur above the critical concentrations (0.175 wt%) corresponding to the nanotube penetration threshold. These materials can be useful in the design of sensors, including sensors that integrate biological species or electrical active chemical properties [94].

Maksiem et al. explained that forming a one-dimensional van der Waals structure composed of two SWCNTs into a DWCNT creates a synergy effect that dramatically affects the optical and electronic characteristics of the two layers.

The sample combined DWCNT absorption, wavelength-dependent infrared fluorescence excitation (PLE), and wavelength-dependent resonance Raman scattering (RRS) spectroscopy. It was obtained by a refined DWCNT ultrasonic treatment or by careful solubilization that strictly avoids electronic classification, both of which eliminate unwanted SWCNTs that can be obscured by density-gradient ultracentrifugation [95]. Lionel et al. considered semiconductor oligomers, i.e., 2,7-bis-(3,3''-didodecyl-[2,2',5',2'';5'',2'''])quaterthiophen-, and applied them as photocell components as a double-walled carbon nanotube (DWCNT) bulk heterojunction. The three-way system (QTF12-DWCNT and PCBM) showed an open voltage ( $V_{oc}$ ) = 0.53 V and a power conversion efficiency of 0.43%. This research can be applied in the fabrication of solar cells, etc. [96]. Levshov et al. performed electron diffraction, Raman scattering experiments, and transmission electron microscopy on individual floating double-walled carbon nanotubes (DWCNTs). The first two techniques enabled a clear determination of the DWCNT structure. This study discussed this discrepancy in terms of the mechanical coupling between the layers of the DWCNTs resulting in a collective vibration mode [97]. Wang et al. manufactured field-effect transistors (FETs) using double-walled carbon nanotubes (DWCNTs). Electrical transmission measurements were then performed on 125 DWCNT FETs. Of these, 52 were found to have, essentially, semiconductor field-effect properties; 44 had metal properties; and 29 had no pure semiconductor or metal properties. In this study, three different types of field-effect properties were identified in the M-S and S-M combinations of two shells: semiconductor (S)-S, metal

(M)-M, and DWCNT. Similar screening effects are also expected to play a significant role in the electron transport of MWCNTs, and their effects are particularly important for larger MWCNTs [98]. Herisanu et al. devoted themselves to the epidemiological investigation of double-walled carbon nanotubes (DWCNTs) that were affected by the Winkler–Pasternak foundation near a primary resonance. An accurate analysis was first reported, taking into account the cumulative effect of the nonlinearity induced simultaneously by the curvature of the beam, the van der Waals forces, the Winkler–Pasternak foundation, and the effects of the discontinuities that were indicated by the presence of Dirac functions. Increasing certain configuration parameters significantly reduces the stability area, all of which have been shown to be of great help in guiding the design of advanced nanoelectromechanical devices where nanotubes act as the primary element [99].

DWCNTs have various characteristics due to their structure; thus, it is believed that they can be applied in various fields, such as nanoelectromechanical devices and the design of sensors that integrate electroactive chemicals or biological species. As mentioned above, DWCNTs are expected to be applicable in electronic conductive sensors, electrochemical sensors, flexible pressure sensors, capacitive pressure sensing, etc.

### 3.4.3. MWCNTs and Their Composites

Multi-walled carbon nanotubes (MWCNTs) are carbon nanotubes with two or more walls. They have good heat or electricity transfer properties, a long extension, are hard, have a similar electricity and thermal conductivity to copper and diamond, and have a strength of approximately 100 times that of steel. Although their physical properties are lower than those of single-walled carbon nanotubes (SWCNTs), they have excellent mechanical properties, thereby facilitating mass synthesis. Research related to MWCNTs includes electrochemical performance, sensors, thin films, electrocatalysts, batteries, etc. [100–105].

A systematization of MWCNT journals with bibliographic sources is listed in Table 7.

**Table 7.** Systematization of MWCNT articles.

Title	Main Content	Applications	Relevant Literature
Pt <sub>2</sub> CeO <sub>2</sub> Heterojunction Supported on Multi walled Carbon Nanotubes for Robust Electrocatalytic Oxidation of Methanol	Multi-walled carbon nanotubes	MWCNT-based electrochemical sensors	Yang et al. [106]
Flexible Room-Temperature Ammonia Gas Sensors Based on PANI-MWCNTs/PDMS Film for Breathing Analysis and Food Safety	PANI-MWCNTs/PDMS	MWCNT-based ammonia gas sensors	Zhu et al. [107]
In Situ Metal Organic Framework (ZIF-8) and Mechano-fusion-Assisted MWCNT Coating of LiFePO <sub>4</sub> /C Composite Material for Lithium-Ion Batteries	MWCNT coating of LiFePO <sub>4</sub> /C composite material	MWCNT-based electrochemical sensors	Mathur et al. [108]
Preparation of Thermoplastic Polyurethane/Multi-Walled Carbon Nanotubes Composite Foam with High Resilience Performance via Fused Filament Fabrication and CO <sub>2</sub> Foaming Technique	Thermoplastic polyurethane/multi-walled carbon nanotube composite	Thermoplastic polyurethane/MWCNT composite foam-based wearable flexible sensors	Guo et al. [109]
Research on Temperature-Switched Dopamine Electrochemical Sensor Based on Thermosensitive Polymers and MWCNTs	Multi-walled carbon nanotubes	Thermosensitive polymer and MWCNT-based temperature-switched dopamine electrochemical sensor	Wang et al. [110]

Yang et al. produced a Pt<sub>2</sub>CeO<sub>2</sub> heterojunction nanocluster for multi-walled carbon nanotubes in a deep eutectic solvent, a special form of ionic liquid. And the catalyst was heat-treated at 400 °C with N<sub>2</sub>. The Pt<sub>2</sub>CeO<sub>2</sub>/CNTs-400 catalyst significantly improved the electrocatalyst performance in the methanol oxidation reaction (MOR) direction when compared to the heat-treated Pt<sub>2</sub>CeO<sub>2</sub>/CNTs-500 (60.3 mA<sub>mgPt</sub><sup>-1</sup>), Pt<sub>2</sub>CeO<sub>2</sub>/CNTs-300

(45.9.2 M MgPt<sup>-1</sup>), and M<sub>2</sub>C<sub>6</sub>Cnt-1 (64S). This study demonstrates a new method for constructing high-performance Pt-CeO<sub>2</sub> catalysts for direct methanol fuel cells (DMFCs). This research can be applied to direct methanol fuel cells, etc. [106]. Zhu et al. grew multi-walled carbon nanotubes (MWCNTs) on top of polydimethylsiloxane (PDMS) films, which were further transformed into polyaniline (PANI) by using chemical oxidation synthesis. The excellent flexibility of the PANI-MWCNT/PDMS films showed stable initial resistance values even under bending conditions. Flexible sensors showed excellent flexible NH<sub>3</sub> detection performance, including low detection limits (10 ppb) at room temperature. The above results show the applicability of PANI-MWCNT/PDMS sensors to monitor NH<sub>3</sub> in human respiration and food [107]. Mathur et al. developed and investigated the ZIF-8 (zeolitic imidazolate) framework and MWCNT (multi-walled carbon nanotube)-modified LiFePO<sub>4</sub>/C (LFP) composite cathode materials in detail. ZIF-8 and MWCNTs can be used as ion- and electron-conductive materials, respectively. This excellent result was obtained mainly from the improvement of the lithium-ion transfer characteristics derived from the synergy between the ZIF-8 coating material and the MWCNT coating material, the low polarization effect, and the interfacial impedance of the LFP-composite cathode material. This research can be applied in energy storage, high-rate lithium-ion battery applications, etc. [108]. Guo et al. manufactured high elastic-foaming sensors by combining additive manufacturing and green physical foaming. The conductive filaments were prepared by the physical method of melt mixing by using TPU with modified MWCNTs. In this study, the sensing characteristics of composite materials were evaluated. And the current signal held steady at different loading speeds and small compressive strains. Using this highly elastic conductive composite material, we designed shoe insoles that successfully detect human walking and other movements [109]. Wang et al. constructed a temperature-controlled electrochemical sensor based on a composite film consisting of temperature-sensitive polymer poly(N-isopropyl acrylate) (PNIPAM) and carboxylated multi-walled carbon nanotubes (MWCNTs-COOH). In addition, it was shown that the temperature sensitivity and reversibility were excellent when dopamine (DA) was detected. In high-temperature environments, the polymer contracts, exposing the electrical active area and increasing the background current. Dopamine can typically perform redox reactions and produce a reaction current indicating an “on” state. This switched sensor provides a new way to apply thermosensitive polymers. This study can be applied to temperature-controlled electrochemical sensors, etc. [110].

MWCNTs have various characteristics due to their structure; thus, it is believed that they can be applied in various fields, such as electricity, chemistry, and machinery. As mentioned above, MWCNTs are expected to be applicable in electrochemical sensors, ammonia gas sensors, wearable flexible sensors, temperature-switched dopamine electrochemical sensors, etc.

#### 4. Summary and Future Prospects

Research on high-tech chemosensor materials is also increasing due to interest in fields such as the Fourth Industrial Revolution, the Internet of Things (IOT), and artificial intelligence (AI). Nanomaterials have the advantage of having a large surface area, thus making it easy to express more efficient characteristics. Furthermore, they have recently been widely applied in various fields. Therefore, in this review, nanomaterials were classified according to their nanostructures (nanograins, nanowires, nanorolls, etc.) and systematically reviewed in depth.

- Current status

Currently, research and introduction cases on nanomaterials are increasing exponentially. Nanomaterials can be used in various fields, such as in body drugs, electrically conductive materials, and flexible displays. The representative materials of nanoparticles include TiO<sub>2</sub>, PDEN, Mo/Fe, Bi<sub>2</sub>MoO<sub>6</sub>, etc. In addition, the representative materials of nanowires include CuNW, AgNW, and GaAsP single nanowires. Moreover, nanoroll-type materials include SWCNTs, DWCNTs, and MWCNTs.

- The main obstacles to be overcome

In the case of nanomaterials, there is a controversy over their harmfulness. In particular, in the case of certain nanomaterials, there has been a controversy over their harmfulness in Europe, resulting in restrictions being put on their exports. An example of a disorder is that, in 2003, NASA's Johnson Space Center research team injected CNT into mice's lungs as a solution, resulting in lung tissue damage. Nanomaterials increase the chances of causing stress at the cell level. They can also affect cardiovascular disease. Therefore, when coating or applying nanomaterials to other objects, it is necessary to select binders well to prevent nanomaterials from escaping. In addition, it is essential to wear protective wear, such as special masks, when processing nanomaterials.

- Future perspectives

As the demand for convergence chemosensor materials increases, more eco-friendly and high-value-added multifunctional nanomaterials are expected to be introduced in the future. In particular, their applications in substances, drug delivery systems, and coating sheets, which maximize functional expression due to their large surface area, is expected to increase.

Having made the points outlined above, I summarize my findings as follows: nanomaterials are expected to contribute greatly to various research fields. In this review, the properties of nanomaterials for chemosensors were divided into structures (nanograins, nanowires, nanorolls, etc.), and the manufacturing methods, characteristics, and application methods were analyzed to provide suggestions for their application in extreme, cutting-edge chemosensor industries.

**Funding:** This research received no external funding.

**Institutional Review Board Statement:** Not applicable.

**Informed Consent Statement:** Not applicable.

**Data Availability Statement:** Not applicable.

**Conflicts of Interest:** The author declares no conflict of interest.

## References

1. Moaser, A.G.; Afkham, A.G.; Khoshnavazi, R.; Rostamnia, S. Nickel substituted polyoxometalates in layered double hydroxides as metal-based nanomaterial of POM-LDH for green catalysis effects. *Sci. Rep.* **2023**, *13*, 4114. [[CrossRef](#)]
2. Lee, D.; Huntoon, K.; Lux, J.; Kim, B.Y.S.; Jiang, W. Engineering nanomaterial physical characteristics for cancer immunotherapy. *Nat. Rev. Bioeng.* **2023**, *1*, 499–517. [[CrossRef](#)]
3. Engel, M.; Farmer, D.B.; Azpiroz, J.T.; Seo, J.-W.T.; Kang, J.; Avouris, P.; Hersam, M.C.; Krupke, R.; Steiner, M. Graphene-enabled and directed nanomaterial placement from solution for large-scale device integration. *Nat. Commun.* **2018**, *9*, 4095. [[CrossRef](#)] [[PubMed](#)]
4. Falinski, M.M.; Plata, D.L.; Chopra, S.S.; Theis, T.L.; Gilbertson, L.M.; Zimmerman, J.B. A framework for sustainable nanomaterial selection and design based on performance, hazard, and economic considerations. *Nat. Nanotechnol.* **2018**, *13*, 708–714. [[CrossRef](#)] [[PubMed](#)]
5. Zhang, G.; Cong, Y.; Liu, F.-L.; Sun, J.; Zhang, J.; Cao, G.; Zhou, L.; Yang, W.; Song, Q.; Wang, F.; et al. A nanomaterial targeting the spike protein captures SARS-CoV-2 variants and promotes viral elimination. *Nat. Nanotechnol.* **2022**, *17*, 993–1003. [[CrossRef](#)] [[PubMed](#)]
6. Abbas, N.; Shatanawi, W.; Shatnawi, T.A.M. Transportation of nanomaterial Maxwell fluid flow with thermal slip under the effect of Soret–Dufour and second-order slips: Nonlinear stretching. *Sci. Rep.* **2023**, *13*, 2182. [[CrossRef](#)] [[PubMed](#)]
7. Zhang, Y.; Zhu, G.; Dong, B.; Wang, F.; Tang, J.; Stadler, F.J.; Yang, G.; Hong, S.; Xing, F. Interfacial jamming reinforced Pickering emulgel for arbitrary architected nanocomposite with connected nanomaterial matrix. *Nat. Commun.* **2021**, *12*, 111. [[CrossRef](#)] [[PubMed](#)]
8. Yan, X.; Sedykh, A.; Wang, W.; Yan, B.; Zhu, H. Construction of a web-based nanomaterial database by big data curation and modeling friendly nanostructure annotations. *Nat. Commun.* **2020**, *11*, 2519. [[CrossRef](#)] [[PubMed](#)]
9. Aubert, T.; Huang, J.-Y.; Ma, K.; Hanrath, T.; Wiesner, U. Porous cage-derived nanomaterial inks for direct and internal three-dimensional printing. *Nat. Commun.* **2020**, *11*, 4695. [[CrossRef](#)] [[PubMed](#)]

10. Nazir, U.; Sohail, M.; Kumam, P.; Elmasry, Y.; Sitthithakerngkiet, K.; Ali, M.R.; Khan, M.J.; Galal, A.M. Thermal and solute aspects among two viscosity models in synovial fluid inserting suspension of tri and hybrid nanomaterial using finite element procedure. *Sci. Rep.* **2022**, *12*, 21577. [[CrossRef](#)]
11. Wei, Y.; Tang, T.; Pang, H.-B. Cellular internalization of bystander nanomaterial induced by TAT-nanoparticles and regulated by extracellular cysteine. *Nat. Commun.* **2019**, *10*, 3646. [[CrossRef](#)] [[PubMed](#)]
12. Shah, Z.; Jafaryar, M.; Sheikholeslami, M.; Kumam, P. Heat transfer intensification of nanomaterial with involve of swirl flow device concerning entropy generation. *Sci. Rep.* **2021**, *11*, 12504. [[CrossRef](#)] [[PubMed](#)]
13. Nguyen, T.T.; Thi, Q.A.N.; Le, N.H.; Nguyen, N.H. Synthesis of a novel porous Ag<sub>2</sub>O nanomaterial on ion exchange resin and its application for COD determination of high salinity water. *Sci. Rep.* **2021**, *11*, 11487. [[CrossRef](#)] [[PubMed](#)]
14. Ryoo, R.; Kim, J.; Jo, C.; Han, S.W.; Kim, J.-C.; Park, H.; Han, J.; Shin, H.S.; Shin, J.W. Rare-earth-platinum alloy nanoparticles in mesoporous zeolite for catalysis. *Nature* **2020**, *585*, 221–224. [[CrossRef](#)] [[PubMed](#)]
15. Chen, Y.; Wu, W.; Gonzalez-Munoz, S.; Forcieri, L.; Wells, C.; Jarvis, S.P.; Wu, F.; Young, R.; Dey, A.; Isaacs, M.; et al. Nanoarchitecture factors of solid electrolyte interphase formation via 3D nano-rheology microscopy and surface force-distance spectroscopy. *Nat. Commun.* **2023**, *14*, 1321. [[CrossRef](#)] [[PubMed](#)]
16. Malm, A.V.; Corbett, J.C.W. Improved Dynamic Light Scattering using an adaptive and statistically driven time resolved treatment of correlation data. *Sci. Rep.* **2019**, *9*, 13519. [[CrossRef](#)] [[PubMed](#)]
17. Jeffries, C.M.; Ilavsky, J.; Martel, A.; Hinrichs, S.; Meyer, A.; Pedersen, J.S.; Sokolova, A.V.; Svergun, D.I. Small-angle X-ray and neutron scattering. *Nat. Rev. Methods Prim.* **2021**, *1*, 70. [[CrossRef](#)]
18. Dalton, K.M.; Greisman, J.B.; Hekstra, D.R. A unifying Bayesian framework for merging X-ray diffraction data. *Nat. Commun.* **2022**, *13*, 7764. [[CrossRef](#)]
19. Wu, L.; Bak, S.; Shin, Y.; Chu, Y.S.; Yoo, S.; Robinson, I.K.; Huang, X. Resolution-enhanced X-ray fluorescence microscopy via deep residual networks. *npj Comput. Mater.* **2023**, *9*, 43. [[CrossRef](#)]
20. Dehghani, M.; Gulvin, S.M.; Flax, J.; Gaborski, T.R. Systematic Evaluation of PKH Labelling on Extracellular Vesicle Size by Nanoparticle Tracking Analysis. *Sci. Rep.* **2020**, *10*, 9533. [[CrossRef](#)]
21. di Polidoro, A.C.; Baghbantarghdari, Z.; De Gregorio, V.; Silvestri, S.; Netti, P.A.; Torino, E. Insulin Activation Mediated by Uptake Mechanisms: A Comparison of the Behavior between Polymer Nanoparticles and Extracellular Vesicles in 3D Liver Tissues. *Biomacromolecules* **2023**, *24*, 2203–2212. [[CrossRef](#)]
22. Cheddah, S.; Xia, Z.; Wang, Y.; Yan, C. Effect of Hydrophobic Moieties on the Assembly of Silica Particles into Colloidal Crystals. *Langmuir* **2023**, *39*, 5655–5669. [[CrossRef](#)] [[PubMed](#)]
23. Lai, C.-F.; Shiau, F.-J. Enhanced and Extended Ophthalmic Drug Delivery by pH-Triggered Drug-Eluting Contact Lenses with Large-Pore Mesoporous Silica Nanoparticles. *ACS Appl. Mater. Interfaces* **2023**, *15*, 18630–18638. [[CrossRef](#)] [[PubMed](#)]
24. Karnwal, A.; Kumar, G.; Pant, G.; Hossain, K.; Ahmad, A.; Alshammari, M.B. Perspectives on Usage of Functional Nanomaterials in Antimicrobial Therapy for Antibiotic-Resistant Bacterial Infections. *ACS Omega* **2023**, *8*, 13492–13508. [[CrossRef](#)] [[PubMed](#)]
25. Luo, W.; Dong, F.; Wang, M.; Li, T.; Wang, Y.; Dai, W.; Zhang, J.; Jiao, C.; Song, Z.; Shen, J.; et al. Particulate Standard Establishment for Absolute Quantification of Nanoparticles by LA-ICP-MS. *Anal. Chem.* **2023**, *95*, 6391–6398. [[CrossRef](#)] [[PubMed](#)]
26. Mao, Y.; Huang, W.; Jia, R.; Bian, Y.; Pan, M.-H.; Ye, X. Correlation between Protein Features and the Properties of pH-Driven-Assembled Nanoparticles: Control of Particle Size. *J. Agric. Food Chem.* **2023**, *71*, 5686–5699. [[CrossRef](#)] [[PubMed](#)]
27. Nicoletta, F.P.; Iemma, F. Nanomaterials for Drug Delivery and Cancer Therapy. *Nanomaterials* **2023**, *13*, 207. [[CrossRef](#)] [[PubMed](#)]
28. Xie, J.; Zhang, J.; Liu, S.; You, Z.; Zhang, Z.; Zhao, T.; Zhang, X.; Wu, R. Developing Mg-Gd-Dy-Ag-Zn-Zr Alloy with High Strength via Nano-Precipitation. *Nanomaterials* **2023**, *13*, 1219. [[CrossRef](#)]
29. Sarasati, A.; Syahrudin, M.H.; Nuryanti, A.; Ana, I.D.; Barlian, A.; Wijaya, C.H.; Ratnadewi, D.; Wungu, T.D.K.; Takemori, H. Plant-Derived Exosome-like Nanoparticles for Biomedical Applications and Regenerative Therapy. *Biomedicines* **2023**, *11*, 1053. [[CrossRef](#)]
30. El-Geassy, A.A.; Halim, K.S.A.; Alghamdi, A.S. A Novel Hydro-Thermal Synthesis of Nano-Structured Molybdenum-Iron Intermetallic Alloys at Relatively Low Temperatures. *Materials* **2023**, *16*, 2736. [[CrossRef](#)]
31. Abbas, S.F.; Bukhari, M.A.; Raza, M.A.S.; Abbasi, G.H.; Ahmad, Z.; Alqahtani, M.D.; Almutairi, K.F.; Abd\_Allah, E.F.; Iqbal, M.A. Enhancing Drought Tolerance in Wheat Cultivars through Nano-ZnO Priming by Improving Leaf Pigments and Antioxidant Activity. *Sustainability* **2023**, *15*, 5835. [[CrossRef](#)]
32. Yan, L.; Tang, J.; Qiao, Q.-A.; Cai, H.; Dong, Y.; Jin, J.; Xu, Y.; Gao, H. Construction and Enhanced Efficiency of Bi<sub>2</sub>MoO<sub>6</sub>/ZnO Compo-Sites for Visible-Light-Driven Photocatalytic Performance. *Nanomaterials* **2023**, *13*, 214. [[CrossRef](#)]
33. Sasaki, M.; Wu, H.; Kawakami, D.; Takaishi, S.; Kajiwara, T.; Miyasaka, H.; Breedlove, B.K.; Yamashita, M.; Kishida, H.; Matsuzaki, H.; et al. Effect of an In-Plane Ligand on the Electronic Structures of Bromo-Bridged Nano-Wire Ni–Pd Mixed-Metal Complexes, [Ni<sub>1-x</sub>Pd<sub>x</sub>(bn)<sub>2</sub>Br]Br<sub>2</sub> (bn = 2S,3S-Diaminobutane). *Inorg. Chem.* **2009**, *48*, 7446–7451. [[CrossRef](#)] [[PubMed](#)]
34. Zeghouane, M.; Grégoire, G.; Chereau, E.; Avit, G.; Staudinger, P.; Moselund, K.E.; Schmid, H.; Coulon, P.-M.; Shields, P.; Goktas, N.I.; et al. Selective Area Growth of GaAs Nanowires and Microplatelet Arrays on Silicon by Hydride Vapor-Phase Epitaxy. *Cryst. Growth Des.* **2023**, *23*, 2120–2127. [[CrossRef](#)]
35. Elalaily, T.; Berke, M.; Kedves, M.; Fülöp, G.; Scherübl, Z.; Kanne, T.; Nygård, J.; Makk, P.; Csonka, S. Signatures of Gate-Driven Out-of-Equilibrium Superconductivity in Ta/InAs Nanowires. *ACS Nano* **2023**, *17*, 5528–5535. [[CrossRef](#)] [[PubMed](#)]

36. Ulrich, N.; Schäfer, M.; Römer, M.; Straub, S.D.; Zhang, S.; Brötz, J.; Trautmann, C.; Scheu, C.; Etzold, B.J.M.; Toimil-Molares, M.E. Cu Nanowire Networks with Well-Defined Geometrical Parameters for Catalytic Electrochemical CO<sub>2</sub> Reduction. *ACS Appl. Nano Mater.* **2023**, *6*, 4190–4200. [[CrossRef](#)]
37. Mao, H.; Chen, J.; He, L.; Fan, Z.; Ren, Y.; Yin, J.; Dai, W.; Yang, H. Halide-Salt-Free Synthesis of Silver Nanowires with High Yield and Purity for Transparent Conductive Films. *ACS Omega* **2023**, *8*, 7607–7614. [[CrossRef](#)]
38. Wang, S.; She, L.; Zheng, Q.; Song, Y.; Yang, Y.; Chen, L. Ag-Doped CuV<sub>2</sub>O<sub>6</sub> Nanowires for Enhanced Visible-Light Photocatalytic CO<sub>2</sub> Reduction. *Ind. Eng. Chem. Res.* **2022**, *62*, 455–465. [[CrossRef](#)]
39. Yalcin, S.E.; Malvankar, N.S. The blind men and the filament: Understanding structures and functions of microbial nanowires. *Curr. Opin. Chem. Biol.* **2020**, *59*, 193–201. [[CrossRef](#)]
40. Jin, H.; Xu, Z.; Hu, Z.-Y.; Yin, Z.; Wang, Z.; Deng, Z.; Wei, P.; Feng, S.; Dong, S.; Liu, J.; et al. Mesoporous Pt@Pt-skin Pt<sub>3</sub>Ni core-shell framework nanowire electrocatalyst for efficient oxygen reduction. *Nat. Commun.* **2023**, *14*, 1518. [[CrossRef](#)]
41. Wakizaka, M.; Kumagai, S.; Wu, H.; Sonobe, T.; Iguchi, H.; Yoshida, T.; Yamashita, M.; Takaishi, S. Macro- and atomic-scale observations of a one-dimensional heterojunction in a nickel and palladium nanowire complex. *Nat. Commun.* **2022**, *13*, 1188. [[CrossRef](#)] [[PubMed](#)]
42. Gu, L.; Poddar, S.; Lin, Y.; Long, Z.; Zhang, D.; Zhang, Q.; Shu, L.; Qiu, X.; Kam, M.; Javey, A.; et al. A biomimetic eye with a hemispherical perovskite nanowire array retina. *Nature* **2020**, *581*, 278–282. [[CrossRef](#)] [[PubMed](#)]
43. Chen, N.; Xiao, T.-H.; Luo, Z.; Kitahama, Y.; Hiramatsu, K.; Kishimoto, N.; Itoh, T.; Cheng, Z.; Goda, K. Porous carbon nanowire array for surface-enhanced Raman spectroscopy. *Nat. Commun.* **2020**, *11*, 4772. [[CrossRef](#)] [[PubMed](#)]
44. Borsoi, F.; Zuo, K.; Gazibegovic, S.; Veld, R.L.M.O.H.; Bakkers, E.P.A.M.; Kouwenhoven, L.P.; Heedt, S. Transmission phase read-out of a large quantum dot in a nanowire interferometer. *Nat. Commun.* **2020**, *11*, 3666. [[CrossRef](#)] [[PubMed](#)]
45. Holm, J.V.; Jørgensen, H.I.; Krogstrup, P.; Nygård, J.; Liu, H.; Aagesen, M. Surface-passivated GaAsP single-nanowire solar cells exceeding 10% efficiency grown on silicon. *Nat. Commun.* **2013**, *4*, 1498. [[CrossRef](#)] [[PubMed](#)]
46. Mocking, T.F.; Bampoulis, P.; Oncel, N.; Poelsema, B.; Zandvliet, H.J.W. Electronically stabilized nanowire growth. *Nat. Commun.* **2013**, *4*, 2387. [[CrossRef](#)] [[PubMed](#)]
47. Curtis, A.; Calvi, C.; Tinsley, J.; Hollinger, R.; Kaymak, V.; Pukhov, A.; Wang, S.; Rockwood, A.; Wang, Y.; Shlyaptsev, V.N.; et al. Micro-scale fusion in dense relativistic nanowire array plasmas. *Nat. Commun.* **2018**, *9*, 1077. [[CrossRef](#)]
48. Liu, Z.; Zhan, Y.; Shi, G.; Moldovan, S.; Gharbi, M.; Song, L.; Ma, L.; Gao, W.; Huang, J.; Vajtai, R.; et al. Anomalous high capacitance in a coaxial single nanowire capacitor. *Nat. Commun.* **2012**, *3*, 879. [[CrossRef](#)]
49. Hwang, A.; Kim, E.; Moon, J.; Lee, H.; Lee, M.; Jeong, J.; Lim, E.-K.; Jung, J.; Kang, T.; Kim, B. Atomically Flat Au Nanoplate Platforms Enable Ultraspecific Attomolar Detection of Protein Biomarkers. *ACS Appl. Mater. Interfaces* **2019**, *11*, 18960–18967. [[CrossRef](#)]
50. Chen, C.; Zhang, N.; Liu, X.; He, Y.; Wan, H.; Liang, B.; Ma, R.; Pan, A.; Roy, V.A.L. Polypyrrole-Modified NH<sub>4</sub>NiPO<sub>4</sub>·H<sub>2</sub>O Nanoplate Arrays on Ni Foam for Efficient Electrode in Electrochemical Capacitors. *ACS Sustain. Chem. Eng.* **2016**, *4*, 5578–5584. [[CrossRef](#)]
51. Choi, D.; Wang, D.; Bae, I.-T.; Xiao, J.; Nie, Z.; Wang, W.; Viswanathan, V.V.; Lee, Y.J.; Zhang, J.-G.; Graff, G.L.; et al. LiMnPO<sub>4</sub> Nanoplate Grown via Solid-State Reaction in Molten Hydrocarbon for Li-Ion Battery Cathode. *Nano Lett.* **2010**, *10*, 2799–2805. [[CrossRef](#)] [[PubMed](#)]
52. Li, H.; Cao, J.; Zheng, W.; Chen, Y.; Wu, D.; Dang, W.; Wang, K.; Peng, H.; Liu, Z. Controlled Synthesis of Topological Insulator Nanoplate Arrays on Mica. *J. Am. Chem. Soc.* **2012**, *134*, 6132–6135. [[CrossRef](#)] [[PubMed](#)]
53. Zhao, M.; Bosman, M.; Danesh, M.; Zeng, M.; Song, P.; Darma, Y.; Rusydi, A.; Lin, H.; Qiu, C.-W.; Loh, K.P. Visible Surface Plasmon Modes in Single Bi<sub>2</sub>Te<sub>3</sub> Nanoplate. *Nano Lett.* **2015**, *15*, 8331–8335. [[CrossRef](#)] [[PubMed](#)]
54. Xu, B.-B.; Wang, L.; Ma, Z.-C.; Zhang, R.; Chen, Q.-D.; Lv, C.; Han, B.; Xiao, X.-Z.; Zhang, X.-L.; Zhang, Y.-L.; et al. Surface-Plasmon-Mediated Programmable Optical Nanofabrication of an Oriented Silver Nanoplate. *ACS Nano* **2014**, *8*, 6682–6692. [[CrossRef](#)] [[PubMed](#)]
55. Dun, C.; Hewitt, C.A.; Huang, H.; Xu, J.; Montgomery, D.S.; Nie, W.; Jiang, Q.; Carroll, D.L. Layered Bi<sub>2</sub>Se<sub>3</sub> Nanoplate/Polyvinylidene Fluoride Composite Based n-type Thermoelectric Fabrics. *ACS Appl. Mater. Interfaces* **2015**, *7*, 7054–7059. [[CrossRef](#)] [[PubMed](#)]
56. Yan, Z.; Bao, Y.; Manna, U.; Shah, R.A.; Scherer, N.F. Enhancing Nanoparticle Electrodynamics with Gold Nanoplate Mirrors. *Nano Lett.* **2014**, *14*, 2436–2442. [[CrossRef](#)] [[PubMed](#)]
57. Liang, D.; Cabán-Acevedo, M.; Kaiser, N.S.; Jin, S. Gated Hall Effect of Nanoplate Devices Reveals Surface-State-Induced Surface Inversion in Iron Pyrite Semiconductor. *Nano Lett.* **2014**, *14*, 6754–6760. [[CrossRef](#)] [[PubMed](#)]
58. Jeong, D.W.; Kim, K.; Lee, G.; Kang, M.; Chang, H.; Jang, A.-R.; Lee, J.-O. Electrochemical Transparency of Graphene. *ACS Nano* **2022**, *16*, 9278–9286. [[CrossRef](#)]
59. Bao, Q.; Loh, K.P. Graphene Photonics, Plasmonics, and Broadband Optoelectronic Devices. *ACS Nano* **2012**, *6*, 3677–3694. [[CrossRef](#)]
60. Nabil, A.; Hendawy, H.A.M.; Abdel-Salam, R.; Ahmed, R.M.; Shawky, A.; Emara, S.; Ibrahim, N. A Green Voltammetric Determination of Molnupiravir Using a Disposable Screen-Printed Reduced Graphene Oxide Electrode: Application for Pharmaceutical Dosage and Biological Fluid Forms. *Chemosensors* **2023**, *11*, 471. [[CrossRef](#)]
61. Budde, H.; Coca-López, N.; Shi, X.; Ciesielski, R.; Lombardo, A.; Yoon, D.; Ferrari, A.C.; Hartschuh, A. Raman Radiation Patterns of Graphene. *ACS Nano* **2015**, *10*, 1756–1763. [[CrossRef](#)]

62. Wang, Y.; Jaiswal, M.; Lin, M.; Saha, S.; Oezylmaz, B.; Loh, K.P. Electronic Properties of Nanodiamond Decorated Graphene. *ACS Nano* **2012**, *6*, 1018–1025. [[CrossRef](#)] [[PubMed](#)]
63. Kumar, B.; Lee, K.Y.; Park, H.-K.; Chae, S.J.; Lee, Y.H.; Kim, S.-W. Controlled Growth of Semiconducting Nanowire, Nanowall, and Hybrid Nanostructures on Graphene for Piezoelectric Nanogenerators. *ACS Nano* **2011**, *5*, 4197–4204. [[CrossRef](#)] [[PubMed](#)]
64. Valencia-Acuna, P.; Rudayni, F.; Rijal, K.; Chan, W.-L.; Zhao, H. Hybrid Heterostructures to Generate Long-Lived and Mobile Photocarriers in Graphene. *ACS Nano* **2023**, *17*, 3939–3947. [[CrossRef](#)] [[PubMed](#)]
65. Chen, W.; Xiao, H.; Zhou, X.; Xu, X.; Jiang, S.; Qin, Z.; Ding, S.; Bian, C.; Liu, Z. Highly Deformable Graphene/Poly(3,4-ethylenedioxythiophene):Poly(styrene Sulfonate) Hydrogel Composite Film for Stretchable Supercapacitors. *ACS Appl. Energy Mater.* **2022**, *5*, 7277–7286. [[CrossRef](#)]
66. Smith, K.; Retallick, A.; Melendrez, D.; Vijayaraghavan, A.; Heil, M. Modeling Graphene–Polymer Heterostructure MEMS Membranes with the Föppl–von Kármán Equations. *ACS Appl. Mater. Interfaces* **2023**, *15*, 9853–9861. [[CrossRef](#)] [[PubMed](#)]
67. Shi, Z.; Ci, H.; Yang, X.; Liu, Z.; Sun, J. Direct-Chemical Vapor Deposition-Enabled Graphene for Emerging Energy Storage: Versatility, Essentiality, and Possibility. *ACS Nano* **2022**, *16*, 11646–11675. [[CrossRef](#)] [[PubMed](#)]
68. Koulouklidis, A.D.; Tasolamprou, A.C.; Doukas, S.; Kyriakou, E.; Ergoktas, M.S.; Daskalaki, C.; Economou, E.N.; Kocabas, C.; Lidorikis, E.; Kafesaki, M.; et al. Ultrafast Terahertz Self-Induced Absorption and Phase Modulation on a Graphene-Based Thin Film Absorber. *ACS Photonics* **2022**, *9*, 3075–3082. [[CrossRef](#)]
69. Lyu, C.; Cheng, C.; He, Y.; Qiu, L.; He, Z.; Zou, D.; Li, D.; Lu, J. Graphene Hydrogel as a Porous Scaffold for Cartilage Regeneration. *ACS Appl. Mater. Interfaces* **2022**, *14*, 54431–54438. [[CrossRef](#)]
70. Schmitt, A.; Vallet, P.; Mele, D.; Rosticher, M.; Taniguchi, T.; Watanabe, K.; Bocquillon, E.; Fève, G.; Berroir, J.M.; Voisin, C.; et al. Mesoscopic Klein-Schwinger effect in graphene. *Nat. Phys.* **2023**, *19*, 830–835. [[CrossRef](#)]
71. Zhao, W.; Wang, S.; Chen, S.; Zhang, Z.; Watanabe, K.; Taniguchi, T.; Zettl, A.; Wang, F. Observation of hydrodynamic plasmons and energy waves in graphene. *Nature* **2023**, *614*, 688–693. [[CrossRef](#)] [[PubMed](#)]
72. Xia, X.; Zhou, F.; Xu, J.; Wang, Z.; Lan, J.; Fan, Y.; Wang, Z.; Liu, W.; Chen, J.; Feng, S.; et al. Unexpectedly efficient ion desorption of graphene-based materials. *Nat. Commun.* **2022**, *13*, 7247. [[CrossRef](#)] [[PubMed](#)]
73. Zhang, Y.; Polski, R.; Thomson, A.; Lantagne-Hurtubise, É.; Lewandowski, C.; Zhou, H.; Watanabe, K.; Taniguchi, T.; Alicea, J.; Nadj-Perge, S. Enhanced superconductivity in spin–orbit proximitized bilayer graphene. *Nature* **2023**, *613*, 268–273. [[CrossRef](#)] [[PubMed](#)]
74. Machín, A.; Cotto, M.; Duconge, J.; Morant, C.; Petrescu, F.I.; Márquez, F. Sensitive and Reversible Ammonia Gas Sensor Based on Single-Walled Carbon Nanotubes. *Chemosensors* **2023**, *11*, 247. [[CrossRef](#)]
75. Han, H. Characteristics and Applicability Analysis of Nanomorphological Structures for Textile Materials: A systematic review. *Proc. Costume Cult Assoc Conf.* **2023**, *7*, 65.
76. Feng, L.; Wu, R.; Liu, C.; Lan, J.; Lin, Y.-H.; Yang, X. Facile Green Vacuum-Assisted Method for Polyaniline/SWCNT Hybrid Films with Enhanced Thermoelectric Performance by Interfacial Morphology Control. *ACS Appl. Energy Mater.* **2021**, *4*, 4081–4089. [[CrossRef](#)]
77. Deng, W.; Deng, L.; Li, Z.; Zhang, Y.; Chen, G. Synergistically Boosting Thermoelectric Performance of PEDOT:PSS/SWCNT Composites via the Ion-Exchange Effect and Promoting SWCNT Dispersion by the Ionic Liquid. *ACS Appl. Mater. Interfaces* **2021**, *13*, 12131–12140. [[CrossRef](#)] [[PubMed](#)]
78. Mariappan, D.D.; Kim, S.; Zhao, J.; Zhao, H.; Muecke, U.; Gleason, K.; Akinwande, A.I.; Hart, A.J. Ultrathin High-Mobility SWCNT Transistors with Electrodes Printed by Nanoporous Stamp Flexography. *ACS Appl. Nano Mater.* **2023**, *6*, 5075–5080. [[CrossRef](#)]
79. Liu, B.; Alamri, M.; Walsh, M.; Doolin, J.L.; Berrie, C.L.; Wu, J.Z. Development of an ALD-Pt@SWCNT/Graphene 3D Nanohybrid Architecture for Hydrogen Sensing. *ACS Appl. Mater. Interfaces* **2020**, *12*, 53115–53124. [[CrossRef](#)]
80. Charoenpakdee, J.; Suntiitirunruang, O.; Boonchui, S. Investigating valley-dependent current generation due to asymmetric energy dispersion for charge-transfer from a quantum dot to single-walled carbon nanotube. *Sci. Rep.* **2023**, *13*, 3105. [[CrossRef](#)]
81. Dehaghani, M.Z.; Yousefi, F.; Seidi, F.; Bagheri, B.; Mashhadzadeh, A.H.; Naderi, G.; Esmaeili, A.; Abida, O.; Habibzadeh, S.; Saeb, M.R.; et al. Encapsulation of an anticancer drug Isatin inside a host nano-vehicle SWCNT: A molecular dynamics simulation. *Sci. Rep.* **2021**, *11*, 18753. [[CrossRef](#)]
82. Kordek-Khalil, K.; Janas, D.; Rutkowski, P. Revealing the effect of electrocatalytic performance boost during hydrogen evolution reaction on free-standing SWCNT film electrode. *Sci. Rep.* **2021**, *11*, 19981. [[CrossRef](#)] [[PubMed](#)]
83. Koh, H.; Chiashi, S.; Shiomi, J.; Maruyama, S. Heat diffusion-related damping process in a highly precise coarse-grained model for nonlinear motion of SWCNT. *Sci. Rep.* **2021**, *11*, 563. [[CrossRef](#)] [[PubMed](#)]
84. Chen, J.-S.; Trerayapiwat, K.J.; Sun, L.; Krzyaniak, M.D.; Wasielewski, M.R.; Rajh, T.; Sharifzadeh, S.; Ma, X. Long-lived electronic spin qubits in single-walled carbon nanotubes. *Nat. Commun.* **2023**, *14*, 848. [[CrossRef](#)] [[PubMed](#)]
85. Jia, F.; Wu, R.; Liu, C.; Lan, J.; Lin, Y.-H.; Yang, X. High Thermoelectric and Flexible PEDOT/SWCNT/BC Nanoporous Films Derived from Aerogels. *ACS Sustain. Chem. Eng.* **2019**, *7*, 12591–12600. [[CrossRef](#)]
86. Fraser, R.A.; Stoeffler, K.; Ashrafi, B.; Zhang, Y.; Simard, B. Large-Scale Production of PMMA/SWCNT Composites Based on SWCNT Modified with PMMA. *ACS Appl. Mater. Interfaces* **2012**, *4*, 1990–1997. [[CrossRef](#)] [[PubMed](#)]
87. Jiang, T.; Wan, P.; Ren, Z.; Yan, S. Anisotropic Polyaniline/SWCNT Composite Films Prepared by in Situ Electropolymerization on Highly Oriented Polyethylene for High-Efficiency Ammonia Sensor. *ACS Appl. Mater. Interfaces* **2019**, *11*, 38169–38176. [[CrossRef](#)] [[PubMed](#)]

88. Chobsilp, T.; Threrujirapapong, T.; Yordsri, V.; Treetong, A.; Inpaeng, S.; Tedsree, K.; Ayala, P.; Pichler, T.; Shi, L.; Muangrat, W. Highly Sensitive and Selective Formaldehyde Gas Sensors Based on Polyvinylpyrrolidone/Nitrogen-Doped Double-Walled Carbon Nanotubes. *Sensors* **2022**, *22*, 9329. [[CrossRef](#)]
89. Barrejón, M.; Zummo, F.; Mikhalchan, A.; Vilatela, J.J.; Fontanini, M.; Scaini, D.; Ballerini, L.; Prato, M. TEGylated Double-Walled Carbon Nanotubes as Platforms to Engineer Neuronal Networks. *ACS Appl. Mater. Interfaces* **2022**, *15*, 77–90. [[CrossRef](#)]
90. Behrouz, M.; Ghatee, M.H. Simulation of a Patterned Core–Shell Double-Walled Carbon Nanotube with an Optimal Heat Capacity as Efficient Thermal Conductivity Modules. *ACS Appl. Nano Mater.* **2022**, *5*, 1542–1552. [[CrossRef](#)]
91. Luo, X.; Wang, Y.; Tian, Z.; Ma, J.; Yu, H.; Xie, Q. Atomic Correlation between Bilayer Graphene and Double-Walled Carbon Nanotubes. *J. Phys. Chem. C* **2022**, *126*, 4030–4036. [[CrossRef](#)]
92. Aziz, A.; Bazbouz, M.B.; Welland, M.E. Double-Walled Carbon Nanotubes Ink for High-Conductivity Flexible Electrodes. *ACS Appl. Nano Mater.* **2020**, *3*, 9385–9392. [[CrossRef](#)]
93. Gordeev, G.; Wasserroth, S.; Li, H.; Flavel, B.; Reich, S. Moiré-Induced Vibrational Coupling in Double-Walled Carbon Nanotubes. *Nano Lett.* **2021**, *21*, 6732–6739. [[CrossRef](#)] [[PubMed](#)]
94. Le Ouay, B.; Lau-Truong, S.; Flahaut, E.; Brayner, R.; Coradin, T.; Laberty-Robert, C. DWCNT-Doped Silica Gel Exhibiting Both Ionic and Electronic Conductivities. *J. Phys. Chem. C* **2012**, *116*, 11306–11314. [[CrossRef](#)]
95. Erkens, M.; Levshov, D.; Wenseleers, W.; Li, H.; Flavel, B.S.; Fagan, J.A.; Popov, V.N.; Avramenko, M.; Forel, S.; Flahaut, E.; et al. Efficient Inner-to-Outer Wall Energy Transfer in Highly Pure Double-Wall Carbon Nanotubes Revealed by Detailed Spectroscopy. *ACS Nano* **2022**, *16*, 16038–16053. [[CrossRef](#)] [[PubMed](#)]
96. Picard, L.; Lincker, F.; Kervella, Y.; Zagorska, M.; DeBettignies, R.; Peigney, A.; Flahaut, E.; Louarn, G.; Lefrant, S.; Demadrille, R.; et al. Composites of Double-Walled Carbon Nanotubes with bis-Quaterthiophene-Fluorenone Conjugated Oligomer: Spectroelectrochemical and Photovoltaic Properties. *J. Phys. Chem. C* **2009**, *113*, 17347–17354. [[CrossRef](#)]
97. Levshov, D.; Than, T.X.; Arenal, R.; Popov, V.N.; Parret, R.; Paillet, M.; Jourdain, V.; Zahab, A.A.; Michel, T.; Yuzyuk, Y.I.; et al. Experimental Evidence of a Mechanical Coupling between Layers in an Individual Double-Walled Carbon Nanotube. *Nano Lett.* **2011**, *11*, 4800–4804. [[CrossRef](#)] [[PubMed](#)]
98. Wang, S.; Liang, X.L.; Chen, Q.; Zhang, Z.Y.; Peng, L.-M. Field-Effect Characteristics and Screening in Double-Walled Carbon Nanotube Field-Effect Transistors. *J. Phys. Chem. B* **2005**, *109*, 17361–17365. [[CrossRef](#)]
99. Herisanu, N.; Marinca, B.; Marinca, V. Nonlinear Vibration of Double-Walled Carbon Nanotubes Subjected to Mechanical Impact and Embedded on Winkler–Pasternak Foundation. *Materials* **2022**, *15*, 8599. [[CrossRef](#)]
100. Roodbari, N.J.; Hosseini, S.R.; Omrani, A. Synthesis, Characterization, and Electrochemical Performance of rGO-MWCNT/Mn-Co-Cu Nanohybrid as Novel Catalyst for Methanol Electrooxidation. *Energy Fuels* **2023**, *37*, 5489–5498. [[CrossRef](#)]
101. Aslam, F.; Shah, A.; Ullah, N.; Munir, S. Multiwalled Carbon Nanotube/Fe-Doped ZnO-Based Sensors for Droplet Electrochemical Detection and Degradation Monitoring of Brilliant Green. *ACS Appl. Nano Mater.* **2023**, *6*, 6172–6185. [[CrossRef](#)]
102. Song, X.; Zhang, Q.; Wu, H.; Guo, S.; Qiu, J. Highly Efficient Dispersion of Individual Multiwalled Carbon Nanotubes by Polylactide in High Elastic State. *Ind. Eng. Chem. Res.* **2023**, *62*, 5042–5050. [[CrossRef](#)]
103. Nguyen, D.-B.; Ha, V.-P.; Vuong, V.-D.; Chien, Y.-H.; Van Le, T.; Chu, C.-Y. Simulation and Verification of the Direct Current Electric Field on Fabricating High Porosity f-MWCNTs Thin Films by Electrophoretic Deposition Technique. *Langmuir* **2023**, *39*, 3883–3894. [[CrossRef](#)] [[PubMed](#)]
104. Kiran, S.; Houda, S.; Yasmin, G.; Shafiq, Z.; Abbas, A.; Manzoor, S.; Syed, A.; Elgorban, A.M.; Zaghoul, N.S.S.; Ashiq, M.N. Facile Synthesis of a Nickel-Based Dopamine MOF/Multiwalled Carbon Nanotubes Nanocomposite as an Efficient Electrocatalyst for the Oxygen Evolution Reaction. *Energy Fuels* **2023**, *37*, 5388–5398. [[CrossRef](#)]
105. Arévalo-Fester, J.; Briceño, A. Insights into Selective Removal by Dye Adsorption on Hydrophobic vs Multivalent Hydrophilic Functionalized MWCNTs. *ACS Omega* **2023**, *8*, 11233–11250. [[CrossRef](#)] [[PubMed](#)]
106. Yang, P.; Wei, X.; Zhang, L.; Dong, S.; Cao, W.; Ma, D.; Ouyang, Y. Pt<sub>2</sub>CeO<sub>2</sub> Heterojunction Supported on Multiwalled Carbon Nanotubes for Robust Electrocatalytic Oxidation of Methanol. *Molecules* **2023**, *28*, 2995. [[CrossRef](#)] [[PubMed](#)]
107. Zhu, C.; Zhou, T.; Xia, H.; Zhang, T. Flexible Room-Temperature Ammonia Gas Sensors Based on PANI-MWCNTs/PDMS Film for Breathing Analysis and Food Safety. *Nanomaterials* **2023**, *13*, 1158. [[CrossRef](#)]
108. Mathur, P.; Shih, J.-Y.; Li, Y.-J.J.; Hung, T.-F.; Thirumalraj, B.; Ramaraj, S.K.; Jose, R.; Karuppiyah, C.; Yang, C.-C. In Situ Metal Organic Framework (ZIF-8) and Mechanofusion-Assisted MWCNT Coating of LiFePO<sub>4</sub>/C Composite Material for Lithium-Ion Batteries. *Batteries* **2023**, *9*, 182. [[CrossRef](#)]
109. Guo, H.; Thirunavukkarasu, N.; Mubarak, S.; Lin, H.; Zhang, C.; Li, Y.; Wu, L. Preparation of Thermoplastic Polyurethane/Multi-Walled Carbon Nanotubes Composite Foam with High Resilience Performance via Fused Filament Fabrication and CO<sub>2</sub> Foaming Technique. *Polymers* **2023**, *15*, 1535. [[CrossRef](#)]
110. Wang, H.; Feng, Z.; Lin, F.; Zhao, Y.; Hu, Y.; Yang, Q.; Zou, Y.; Zhao, Y.; Yang, R. Research on Temperature-Switched Dopamine Electrochemical Sensor Based on Thermosensitive Polymers and MWCNTs. *Polymers* **2023**, *15*, 1465. [[CrossRef](#)]

**Disclaimer/Publisher’s Note:** The statements, opinions and data contained in all publications are solely those of the individual author(s) and contributor(s) and not of MDPI and/or the editor(s). MDPI and/or the editor(s) disclaim responsibility for any injury to people or property resulting from any ideas, methods, instructions or products referred to in the content.